



The Effects of an Unsteady Reduced Gravity Environment on the Soldering Process

Peter M. Struk
Glenn Research Center, Cleveland, Ohio

Richard D. Pettegrew and Robert S. Downs
National Center for Microgravity Research, Cleveland, Ohio

J. Kevin Watson
Johnson Space Center, Houston, Texas

The NASA STI Program Office . . . in Profile

Since its founding, NASA has been dedicated to the advancement of aeronautics and space science. The NASA Scientific and Technical Information (STI) Program Office plays a key part in helping NASA maintain this important role.

The NASA STI Program Office is operated by Langley Research Center, the Lead Center for NASA's scientific and technical information. The NASA STI Program Office provides access to the NASA STI Database, the largest collection of aeronautical and space science STI in the world. The Program Office is also NASA's institutional mechanism for disseminating the results of its research and development activities. These results are published by NASA in the NASA STI Report Series, which includes the following report types:

- **TECHNICAL PUBLICATION.** Reports of completed research or a major significant phase of research that present the results of NASA programs and include extensive data or theoretical analysis. Includes compilations of significant scientific and technical data and information deemed to be of continuing reference value. NASA's counterpart of peer-reviewed formal professional papers but has less stringent limitations on manuscript length and extent of graphic presentations.
- **TECHNICAL MEMORANDUM.** Scientific and technical findings that are preliminary or of specialized interest, e.g., quick release reports, working papers, and bibliographies that contain minimal annotation. Does not contain extensive analysis.
- **CONTRACTOR REPORT.** Scientific and technical findings by NASA-sponsored contractors and grantees.

- **CONFERENCE PUBLICATION.** Collected papers from scientific and technical conferences, symposia, seminars, or other meetings sponsored or cosponsored by NASA.
- **SPECIAL PUBLICATION.** Scientific, technical, or historical information from NASA programs, projects, and missions, often concerned with subjects having substantial public interest.
- **TECHNICAL TRANSLATION.** English-language translations of foreign scientific and technical material pertinent to NASA's mission.

Specialized services that complement the STI Program Office's diverse offerings include creating custom thesauri, building customized databases, organizing and publishing research results . . . even providing videos.

For more information about the NASA STI Program Office, see the following:

- Access the NASA STI Program Home Page at <http://www.sti.nasa.gov>
- E-mail your question via the Internet to help@sti.nasa.gov
- Fax your question to the NASA Access Help Desk at 301-621-0134
- Telephone the NASA Access Help Desk at 301-621-0390
- Write to:
NASA Access Help Desk
NASA Center for Aerospace Information
7121 Standard Drive
Hanover, MD 21076



The Effects of an Unsteady Reduced Gravity Environment on the Soldering Process

Peter M. Struk
Glenn Research Center, Cleveland, Ohio

Richard D. Pettegrew and Robert S. Downs
National Center for Microgravity Research, Cleveland, Ohio

J. Kevin Watson
Johnson Space Center, Houston, Texas

Prepared for the
42nd Aerospace Sciences Meeting and Exhibit
sponsored by the American Institute of Aeronautics and Astronautics
Reno, Nevada, January 5–8, 2004

National Aeronautics and
Space Administration

Glenn Research Center

This report contains preliminary findings, subject to revision as analysis proceeds.

Trade names or manufacturers' names are used in this report for identification only. This usage does not constitute an official endorsement, either expressed or implied, by the National Aeronautics and Space Administration.

Available from

NASA Center for Aerospace Information
7121 Standard Drive
Hanover, MD 21076

National Technical Information Service
5285 Port Royal Road
Springfield, VA 22100

Available electronically at <http://gltrs.grc.nasa.gov>

THE EFFECTS OF AN UNSTEADY REDUCED GRAVITY ENVIRONMENT ON THE SOLDERING PROCESS

Peter M. Struk
National Aeronautics and Space Administration
Glenn Research Center
Cleveland, Ohio 44135

Richard D. Pettegrew* and Robert S. Downs
National Center for Microgravity Research
Cleveland, Ohio 44135

J. Kevin Watson†
National Aeronautics and Space Administration
Johnson Space Center
Houston, Texas 77058

ABSTRACT

An improved understanding of the effects of reduced gravity is important to applications of soldering during both current and future human space missions. Recently, we conducted a series of manual soldering experiments aboard NASA's KC-135 reduced gravity aircraft. This paper focuses on the interpretation of the unsteady (g-jitter) acceleration environment measured aboard the aircraft as it affects the experimental results. The results presented here use a through-hole geometry that was soldered with the same hardware that is currently on orbit aboard the International Space Station. As presented elsewhere, we observed significant changes in porosity and geometry of solder joints formed in reduced gravity. Based on acceleration measurements during periods when the solder was molten, we examined a data filtering technique to determine the influence of g-jitter on our data. The results of this filter indicate that joint geometry is largely unaffected by the unsteady variations in acceleration as seen aboard the KC-135. We deduced that the increase in voids observed in low gravity can be described by decreases in buoyancy driven bubble motion. An acceleration environment which oscillates about zero gravity further increases joint porosity by keeping bubbles within the joint. Additionally, by examining some partial gravity results we observed that acceleration levels near Martian levels and higher result in porosity data sets similar to our normal gravity results. This suggests the existence of a "threshold" acceleration level below which gravitational effects become important for joint porosity in the through-hole geometry. The techniques and interpretations presented in this paper

may be beneficial to others using the KC-135 research aircraft.

INTRODUCTION

Human space exploration missions beyond low-Earth orbit will be increasingly challenged by limited, or non-existent, re-supply capabilities and constraints on the mass and volume of spares that can be carried. A potential approach for dealing with these concerns for maintenance of electronic equipment is to implement repair at the component level. This would be a significant step beyond the approach employed on the International Space Station (ISS) where electronic repairs are typically accomplished by removal and replacement of complete assemblies or, in limited cases, by removal and replacement of circuit cards. Component-level repair is the approach used by the U.S. Navy for repair of electronics at sea. Among the issues to be addressed before implementation of component-level repair is the potential influence of reduced-gravity environments on the soldering process which represents an essential element of this type of repair.

Several soldering experiments have been conducted onboard the Space Shuttle as "Get Away Special" experiments – operating autonomously in the unpressurized payload bay.¹ The limited results available from these experiments demonstrated dominance of surface tension and increased entrapment of flux. A manual soldering experiment was performed on STS-57 in 1993. Interesting qualitative observations made by the crewmember who performed the test included a perception that the solder joint fillets were more convex than those experienced when soldering in a normal gravity environment and that the solder alloy appeared to solidify more slowly.²

*AIAA Member, Associate Staff Scientist

†AIAA Member, Aerospace Engineer

Since 2001, an ongoing research effort to develop an in-depth understanding of the influence of reduced gravity environments on the manual soldering process is being conducted jointly by The National Center for Microgravity Research (NCMR), NASA Glenn Research Center (GRC), and NASA Johnson Space Center (JSC). The low gravity portion of this effort being conducted on NASA's KC-135 research aircraft uses soldering hardware identical to that currently available onboard the International Space Station (ISS). The experiment involves manual soldering by a contingent of test operators including both highly skilled technicians and less skilled individuals to provide a skill mix that might be encountered in space mission crews. Emphasis has been placed on plated-through-hole device geometries although a limited amount of work has been performed with surface mount devices. Post-flight analysis (done jointly at NASA Glenn and NASA Johnson) consists of a visual inspection, photography, and leg-length measurements of the soldered joints. The cross-sections of the joints are prepared and examined using standard metallographic techniques to obtain porosity measurements. Preliminary findings indicate significant changes in joint porosity and joint geometry in reduced gravity.^{3,4} The differences observed with test operator variation are presented elsewhere.³ This paper focuses on the interpretation of the unsteady acceleration environment aboard the aircraft termed "g-jitter" as it affects the solder joint characteristics.

EXPERIMENT OVERVIEW

A detailed description of the experiment is presented elsewhere³ and only a general description is given here. The experimental apparatus provides accommodations for a test operator, who is strapped to a seat, to manually solder on a circuit board in an enclosed glove box. The soldering iron is a Weller[®] TCP 12P with a PTP7 tip and is the same model as currently flown in the soldering kit aboard the International Space Station. A "plated through-hole" configuration (Figure 1) has been used as the standard test configuration.

Low Gravity Generation

Flying an aircraft (NASA's KC-135) in a parabolic trajectory generates the reduced gravity environment.^{5,6,7,8} The maneuver starts with a full power climb, after which the nose is lowered to trace a parabolic arc. From the time that the nose begins to lower, until the pullout (from the ensuing 'dive' on

the back side of the trajectory), the experiment and crew experience a period of 'reduced gravity', relative to their surroundings. The aircraft is capable of flying reduced gravity parabolas where the targeted acceleration levels are near 0-g_e or higher (i.e. partial-gravity parabolas). The symbol g_e is the gravitational acceleration at the Earth's surface. Typical partial-gravity parabolas include "Lunar" and "Martian" parabolas, which target accelerations of 0.16-g_e and 0.38-g_e, respectively. While the acceleration levels experienced during these maneuvers are near the targeted values, variations due to pilot adjustment (e.g. rotation of the aircraft about its center of gravity) and other residual motions do occur (e.g. engine vibrations, weather).

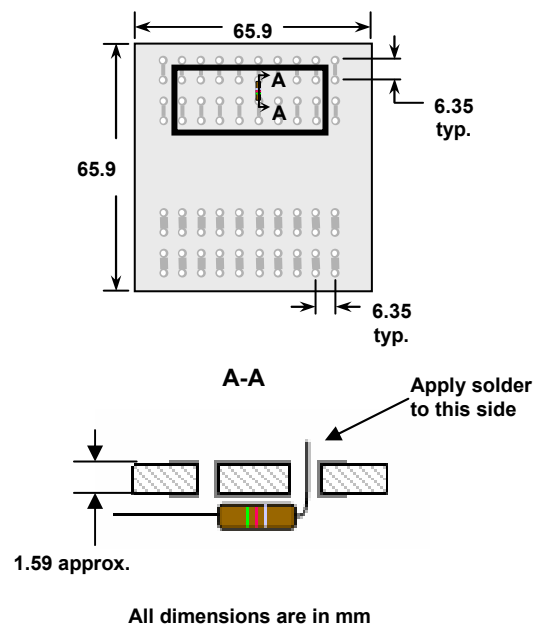


Figure 1. Plated through-hole sample configuration used during recent reduced gravity testing.

Accelerometer and Thermocouple Data

The local acceleration was measured using a 3-axis accelerometer provided by the Space Acceleration Measurement System (SAMS) program at NASA GRC.⁹ The hardware consisted of a single Triaxial Sensor Head (TSH) which houses the accelerometers and is mounted about 30 cm behind the circuit board and at the same height vertically. A Control and Data Unit (CDU) recorded the data generated by the TSH at a 100Hz sampling rate and combined with various filters provided a resolution of disturbances up to 26.2 Hz. We desired to capture low-frequency disturbances (i.e. "DC" level accelerations) since it was expected that higher frequency disturbances

would minimally impact our results. The CDU also recorded analog signals from a pressure transducer and, on select joints, thermocouple (TC) measurements at a collection rate of 30 Hz that were subsequently correlated with video data. This system automatically collected data during each parabola using an algorithm developed by the SAMS team which looked for a sequence of acceleration events that indicated the beginning of a parabola.¹⁰ Specifically, this algorithm looks for a sequence of g-RMS values (root-mean square of all 3 axis) which are calculated every 20th sample (i.e. every 0.2 seconds). The sequence is a g-RMS level below 0.7 g_e for 5 samples (1 second) followed by 3 samples (0.6 seconds) below 0.4 g_e. These numbers were developed based on data taken over many flights aboard the KC-135 and constitute the best compromise for a capability to automatically detect entry into a parabola given the rather noisy acceleration environment on the aircraft.

Figure 2 shows the measured acceleration (relative to normal gravity) for each aircraft axis during a representative zero gravity parabola flown by the KC-135 along with temperature data for the solder joint completed during this parabola. The horizontal lines in each of the top 3 acceleration plots represent ± 0.02 g_e. It is apparent from the graphs that the acceleration oscillates primarily in the vertical axis as the pilots adjust the aircraft to remain near 0-g_e. The other axes show some deviations from 0-g_e especially earlier and later in the parabola. The colored regions in Figure 2 correspond to the soldering events determined from video imaging. The yellow region corresponds to heating of the joint (i.e. when the soldering iron was in contact with the joint). The gray region corresponds to the time interval when

solder was added to the joint. Finally, the blue region corresponds to the cool down period until the joint solidified as judged by the video data. The accuracy of each soldering event measured from video was ± 1 video frame (1/30th of a second) except for joint solidification which often occurred over several frames and occasionally was not detectable from the video. On select joints, a k-type thermocouple (0.002" wire diameter) was spot welded to the circuit board pad prior to testing to obtain heating and cooling profiles of the solder joint. The temperature data for the joint shown in Figure 2 correlates well with observed video data (as indicated by comparing the colored regions with the temperature traces).

EXPERIMENTAL RESULTS

To date, this experiment has generated 971 solder samples in the PTH configuration, including 622 low-gravity samples (including some partial-gravity samples) and 349 normal-gravity samples. Testing was performed during 6 flight-weeks and used seven test operators. Results from the first 3 flight weeks are included here with more complete data sets presented elsewhere^{3,4} and others to be published in the future. The influence of different test operators was discussed in a preliminary fashion in these earlier articles. The primary test conditions for the first 3 flight weeks were:

1. 60/40 Pb/Sn solder with a flux core;
2. 60/40 Pb/Sn solder with a flux core (repeat of flight week 1); and
3. 60/40 Pb/Sn solder, solid-core, with externally applied liquid flux.

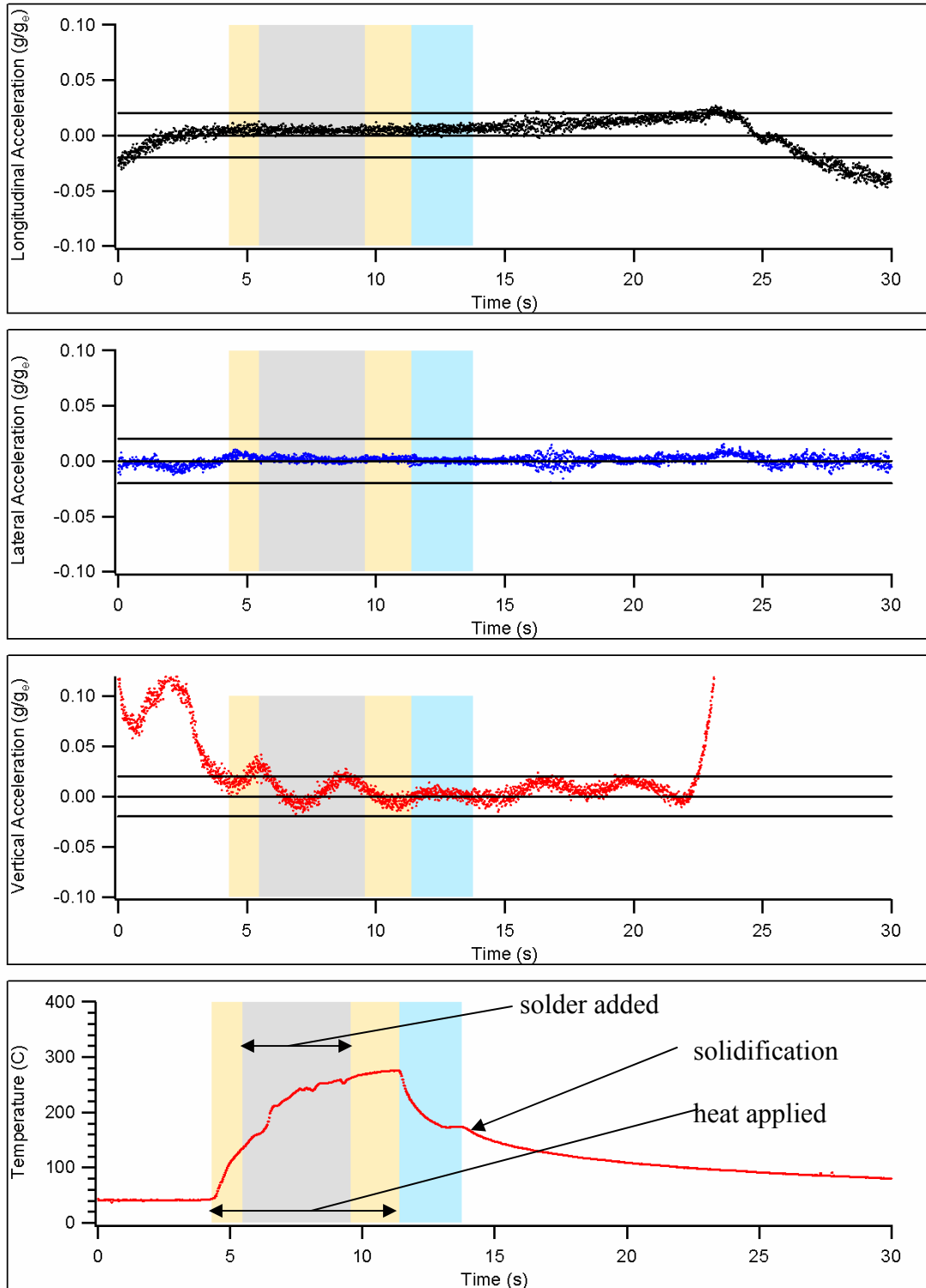


Figure 2. Acceleration data from the SAMS 3-axis accelerometer and temperature data from a thermocouple taken while soldering a PTH joint during a reduced gravity parabola.

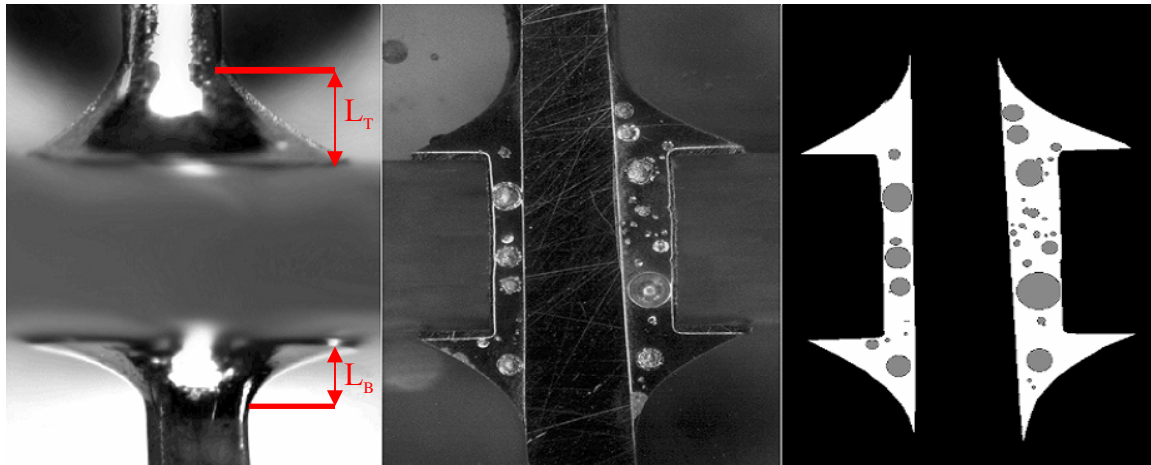


Figure 3. Images of joints after soldering in reduced gravity (left), after cross-sectioning (middle), and after computer analysis (right). Solder was applied to the joint from the top of solder joint as orientated in the images. This joint shows significant sub-surface voids.

Leg Length Ratios

Each sample was photographed (Figure 3, left) and both the top leg length (L_T) and bottom leg length (L_B) was measured. The ratio of leg lengths, L_T / L_B , is shown in Table 1 for each flight week. The table shows that the joint geometry changes when comparing joints soldered in reduced gravity compared with normal gravity. In reduced gravity, the ratio L_T / L_B is higher than unity while in normal gravity this ratio falls below 1. All reduced gravity tests were conducted with the circuit board at approximately a 53° angle relative to the horizontal to facilitate test operator visibility. The orientation does not affect the results because of the reduced gravity environment. During the first flight week, the normal gravity tests were also conducted with the circuit board oriented at the 53° angle. For all subsequent flight weeks, the gravitation direction was oriented perpendicular to the circuit board (top to bottom in Figure 3). Consequently, flight week 1 had leg length ratios closer to 1 compared with subsequent normal gravity tests.

Porosity

Solder joints were examined for internal porosity by mounting the samples in metallographic mounts and

grinding them down to approximately the centerline of the resistor lead. The percentage of porosity was calculated from images ($\sim 20X$ magnification) of these cross-sectioned joints (Figure 3, center). A custom computer program assisted in a manual measurement of the pore area as seen in Figure 3, right. This technique is similar to ASTM Standard E1245-00¹¹, which addresses measurements of inclusions or second-phase constituents. We calculated a porosity percentage by dividing the pore area by the total area of solidified solder in the sample cross-section. This technique was carried out for the majority of both normal gravity and reduced gravity samples. Table 2 shows the mean porosity values for each of the first 3 flight weeks. The uncertainty reflects a 95% confidence interval assuming a normal distribution for the porosity distribution. While the histograms of porosity (i.e. Figure 7 from reference 3) are not Gaussian, a normal distribution assumption for the confidence interval is valid for large sample sizes.¹² Figure 4 shows a plot of the cumulative fraction of samples that have a given porosity or less. For example, this plot shows that 80% of the normal gravity samples (solid red line) have 5% or less porosity, while only about 33% of the 0-g_e samples (solid blue line) have the similar porosity.

Flight Week	Total Samples (0 g _c)	L _T /L _B Complete Data Set (mean ± 95% CI) (0 g _c)	Samples Passing Filter (0 g _c)	L _T /L _B Passing Data Set (0 g _c)	Total Samples (1 g _c)	L _T /L _B Complete Data Set (mean ± 95% CI) (1 g _c)
1	149	1.18 ± 0.08	10	1.25 ± 0.42	59	0.87 ± 0.07
2	112	1.15 ± 0.10	43	1.14 ± 0.21	77	0.74 ± 0.06
3	153	1.21 ± 0.09	103	1.20 ± 0.11	63	0.70 ± 0.13

Table 1. Average leg length ratios (L_T / L_B) for each flight week. The uncertainty reflects a 95% confidence interval assuming a normal distribution for the leg length ratio.

Flight Week	Total Samples Analyzed (0 g _c)	Mean Porosity (%) Complete Data Set (0 g _c)	Samples Passing Filter (0 g _c)	Mean Porosity (%) Passing Data Set (0 g _c)	Mean Porosity (%) Failing Data Set (0 g _c)	Total Samples Analyzed (1 g _c)	Mean Porosity (%) Complete Data Set (1 g _c)
1	114	8.5 ± 1.6	10	7.9 ± 6.7	8.5 ± 1.7	54	3.6 ± 1.9
2	60	12.6 ± 2.7	43	12.5 ± 2.9	12.9 ± 6.3		
3	155	6.4 ± 1.3	103	6.1 ± 1.4	6.9 ± 2.7	57	3.2 ± 1.1

Table 2. Mean porosity measurements for each flight week.

Flight Week	Average RMS g/g _c value for passing data	Average RMS g/g _c value for failing data
1	0.018 ± 0.002	0.064 ± 0.035
2	0.013 ± 0.003	0.038 ± 0.013
3	0.015 ± 0.003	0.043 ± 0.066

Table 3. g-RMS values for the passing data set for each flight week (± 1 standard deviation).

Acceleration Environment – Good vs. Bad Parabolas

Our acceleration measurements indicate that acceleration levels oscillate between ± 0.02 g_c aboard the KC-135 during what we term “quality” reduced gravity portions of a parabola. In Figure 2, this period occurs between roughly 6 and 22 seconds after the beginning of the reduced gravity portion of the parabola. For this experiment, we conjecture that these variations in acceleration would be most important during periods when the solder is in a molten state (from the beginning of the gray to the end of the blue region in Figure 2). To explore the

effect of this unsteady acceleration environment, we calculated an average RMS value of the acceleration magnitude during the period when the solder was molten. The data with acceleration levels less than an average g-RMS value of 0.02 g_c was placed in a separate subset. The average g-RMS values for both the passing and failing subset are shown in Table 3. The results of this filter when applied to the leg length ratios, L_T / L_B, and porosity data are shown in Table 1 and 2, respectively. Almost all of the data from flight week 1 was eliminated from the sample set because the test operators started soldering the joints prior to the portion of the parabola where

acceleration decreased to less than RMS 0.02 g_e . This observation was very important and would not have been discovered had we not made local acceleration measurements. Interestingly, the data filters show minimal effect on the mean values of leg length ratio. The final joint configuration was likely more influenced by later acceleration values (which were typically in the “quality” region) when the joint solidified. With the exception of the first flight week, the mean porosity was also largely unaffected by the acceleration variations. Due to the small numbers of passing samples from flight week 1 and failing samples from flight week 2, we combined the data from the first and second flight weeks which shared the same test conditions. The effect of the acceleration filtering becomes apparent when looking at Figure 4. In this figure, the dashed blue line represents the total “0- g_e ” data set and the solid blue line represents the filtered “0- g_e ” data set. The significant shift in the cumulative distribution function highlights the effect of application of the RMS 0.02 g_e filter and was due almost entirely to flight week 1 data. The cumulative distribution functions showed almost no change when applying the filter to flight weeks 2 and 3 independently (graphs not shown). Thus, if the soldering (particularly the molten period) took place during the

“quality” portion of the parabola, then g-jitter effects showed minimal impact on our results.

Partial Gravity Results

During flight week 2, several parabolas were flown with target acceleration levels of 0.1- g_e , 0.16- g_e (Lunar), and 0.38- g_e (Martian). Although not shown here, these parabolas oscillated about the target acceleration values. For 0.1- g_e parabolas, the amplitudes of oscillation were roughly $\pm 0.02 g_e$ during “quality” periods which was similar to the 0- g_e parabolas. The amplitudes of oscillation increased for the higher targeted acceleration values with the Martian parabolas oscillating between 0.3 and 0.4 g_e . The higher acceleration parabolas, however, did not have any acceleration that could change the bubble direction in the vertical axis (i.e. the acceleration did not pass through zero). The porosity of these joints was measured and the results plotted as a cumulative distribution function for each acceleration level (Figure 5). While the data sets are small (the sample numbers shown in the parenthesis in the legend), the cumulative distributions fall, as expected, between the low gravity and normal gravity results.

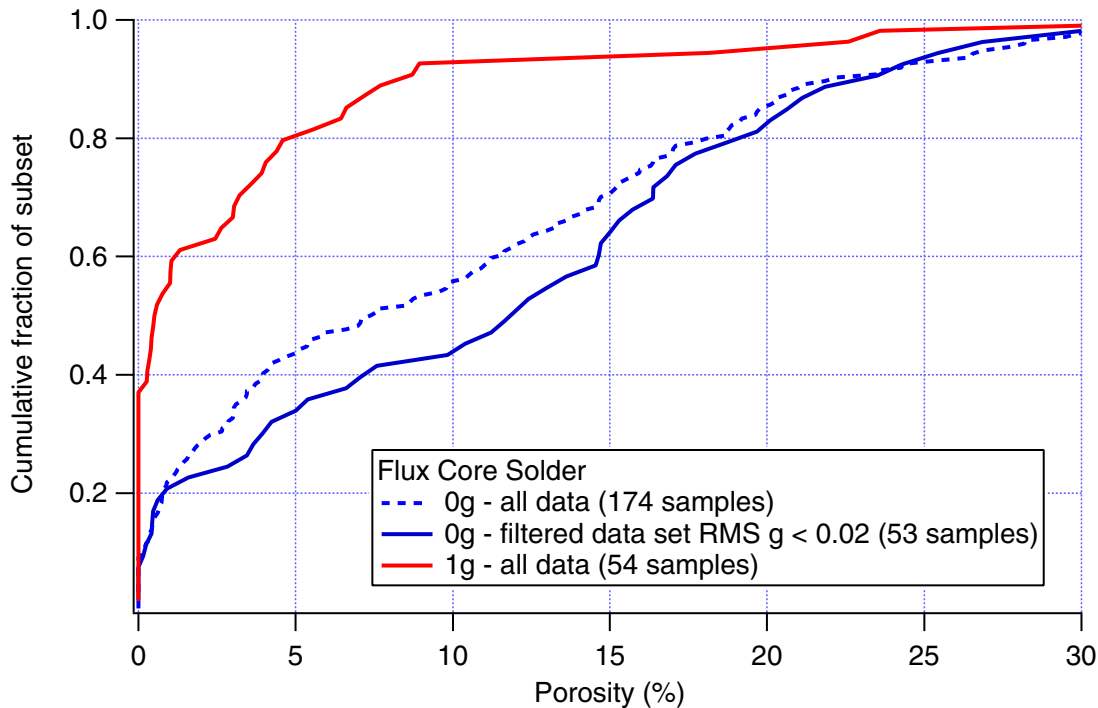


Figure 4. Cumulative distribution function of porosity in solder joints for normal and reduced gravity conditions (filtered and unfiltered).

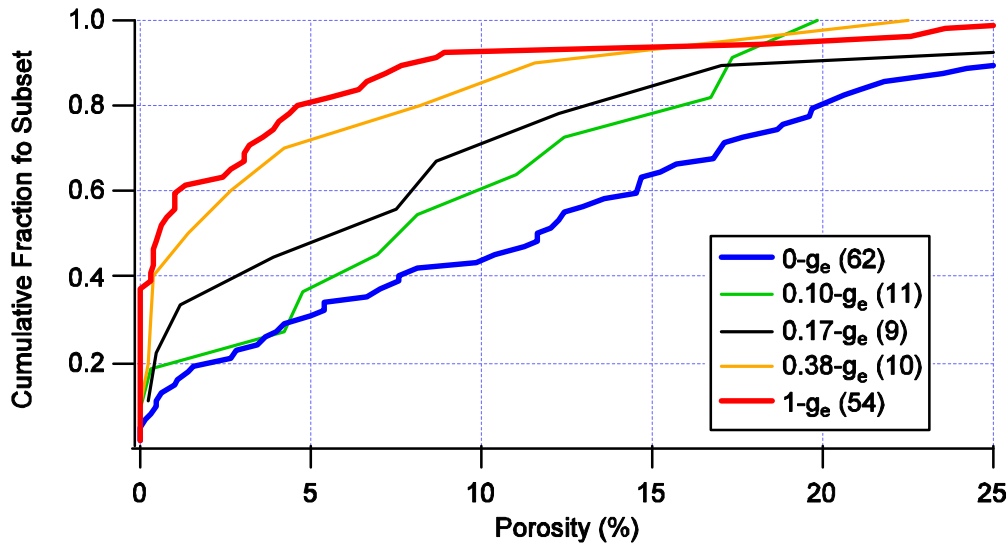


Figure 5. Cumulative distribution function of porosity in solder joints in partial gravity compared with normal and reduced gravity results.

DISCUSSION

Influence of Acceleration: Bubble Motion and Fluid Scaling Arguments

Data like that shown in Figure 2 allows detailed interpretation of the influence of g-jitter on the soldering process. Previously, we conjectured that g-jitter effects would be most important when molten solder is present (i.e. beginning of gray region to end of blue region in Figure 2). Through consideration of some fundamental transport and scaling arguments, we attempt to interpret some of the experimental observations. Fluid transport processes in soldering are complex involving surface tension driven flows, body forces, two-phase flows (bubbles), heat transfer, and phase change. While the dynamics of the wetting process are of interest, the emphasis here will be on the final joint configuration. Soldering in reduced gravity may influence the final joint configuration by:

1. Increasing joint porosity due to entrapped bubbles,
2. Modifying the macroscopic geometry, and
3. Modifying the microstructure.

Gas bubbles, perhaps composed of vaporized flux and/or water vapor, are commonly observed to be present within solder joints. These bubbles, or voids, which appear when the solder joint is molten, are entrapped upon joint solidification (see Figure 3, center). A decrease in gravity reduces the buoyancy force allowing fewer bubbles to escape to the surface

prior to joint solidification thus increasing the porosity of the joint. This effect was clearly demonstrated in reduced gravity testing aboard the KC-135 (Figure 4).

First, we consider only the motion of a bubble in a quiescent fluid. Sy et al.^{13,14} and Morrison and Stewart¹⁵ analyzed the *initial* motion of fluid spheres (e.g. voids or bubbles) within another fluid (e.g. molten solder). Their analysis is valid for a bubble sufficiently far from a wall, assumes non-contaminated surfaces (constant surface tension), constant body force, and creeping flow ($Re^* \ll 1$). While not all of these assumptions are valid for our problem, it is informative to consider their results. According to their results (as can be seen in Figure 11.6 in Clift et al.¹⁶), the characteristic time to reach 50% of the bubble's terminal velocity is approximately $0.25 a^2/\nu$ where "a" is the bubble radius and ν is the kinematic viscosity of the molten solder. Thermo-physical property values used is this and later calculations are shown in Table 4. Using an average bubble radius measured from the PTH configuration of 0.05 mm and the kinematic viscosity of solder, a bubble requires 3×10^{-4} seconds to reach 50% of its terminal velocity – thus, a bubble of this size has likely reached its terminal velocity during the 1-2 seconds of $\pm 0.02 g_e$ excursions on the KC-135. Although a detailed analysis on bubble motion

* The Reynolds number, Re , is based on the bubble diameter and viscosity of the molten solder.

with continually changing g-levels has not been conducted it is probably reasonable to assume that, because of these short transient times, the bubbles motion traces a path parallel to the instantaneous acceleration vector.

Property	Value
ν - kinematic viscosity (553K)	$1.98 \times 10^{-6} \text{ m}^2/\text{s}$
ρ - density (same as solid)	8500 kg/m^3
α - thermal diffusivity	$3.9 \times 10^{-5} \text{ m}^2/\text{s}$
σ - surface tension (extrapolated to 533K)	$4.81 \times 10^{-1} \text{ N/m}$
$\frac{\partial \sigma}{\partial T}$	$-1.3 \times 10^{-4} \text{ N/m/K}$
β -volumetric thermal expansion coefficient	$2.3 \times 10^{-5} \text{ K}^{-1}$

Table 4. Thermo-physical property values for molten Pb/Sn solder taken from a Tin Research Institute Publication.¹⁷

Using the classic analysis of Stokes¹⁸, the terminal velocity, U_T , assuming $1 g_e$, is approximately 3 mm/s ($Re \sim 0.1$). A characteristic length, L , for a bubble to reach the air / solder interface would be the solder board thickness of 1.6 mm (Figure 3, left). Therefore, it is likely that a significant fraction of bubbles have escaped from the PTH joints in normal gravity during the several seconds when the solder is molten. With acceleration levels experienced on the KC-135 ($0.02 g_e$), U_T drops significantly to 0.06mm/s ($Re \sim 0.003$) which suggests (neglecting other fluid motions) that more bubbles will remain in the molten solder up to solidification. It is likely that the oscillating g-environment with a 0-mean further reduces the “net” buoyant transport of bubbles from the joint. This statement is supported by data in Table 2 and Figure 4. During flight week 1, the joints were soldered very early in the parabola while there were still vertical accelerations (i.e. before the “quality” portion of the parabola) and consequently shows significantly lower porosity. In partial gravity, U_T is 0.3, 0.5, and 1.1 mm/s for 0.1 g_e , Lunar, and Martian acceleration levels, respectively. Given a time period on the order of seconds, these velocities suggest that acceleration levels near Martian or higher should generate enough buoyant velocity to eliminate significant porosity in the joints (characteristic length \sim mm) – this is supported by the data presented in Figure 5.

We now consider natural convection fluid flows in the molten solder which can assist in transport of

bubbles and may influence the microstructure of the solidified joint by enhancing fluid transport within the molten liquid. The Grashof Number, Gr , indicates the ratio of buoyant force to the viscous forces (equation 1).

$$Gr = \frac{g\beta\Delta TR^3}{\nu^2} \quad (1)$$

In equation 1, g is the gravitational body acceleration (i.e. $0.02 g_e$ aboard the KC-135), β is the volumetric thermal expansion coefficient of the molten solder, ΔT is the driving temperature difference, R is a characteristic length appropriate for the geometry (0.3 mm for PTH), and ν is the kinematic viscosity. The selection of the annulus radius rather than the circuit board length for the length scales is thought to be appropriate given the small magnitude of Gr and the small Prandtl number of the molten solder.¹⁹ For this calculation, the driving temperature difference was assumed to be 10 K (estimated temperature difference between bulk solder and the adjoining wall – metal lead in this case). In the case of the PTH geometry in normal gravity, Gr is calculated to be of the order 10^{-2} , whereas on the KC-135, Gr is of the order 10^{-4} . A characteristic velocity for such a flow (balancing buoyant and viscous forces) is on the order of 0.1 mm/s in normal gravity which is an order of magnitude smaller than the bubble rise velocity. Thus, with regard to bubble motion, free-convection in the molten solder is likely negligible even at normal gravity for PTH length scales. The influence of small convective flows on microstructure, however, has not been evaluated here.

Reductions in body forces also play an important role in determining the shape of the solder joint. This effect was observed by the changes in leg lengths ratios, L_T / L_B , from normal to reduced gravity as shown in Table 1. Using a characteristic length ($L = 1.6$ mm) of the circuit board (for a hydrostatic pressure difference), a Bond number, Bo (equation 2), can describe the observed difference in leg length ratio of a PTH solder joint when soldering in a reduced gravity environment versus normal gravity.

$$Bo = \frac{\rho L^2 g}{\sigma} \quad (2)$$

In equation 2, ρ is the density of the molten solder and σ is the surface tension force of the molten solder. The Bond number, which is the ratio of gravitational to surface tension forces, is of the

order 1 for the PTH configuration in normal gravity conditions. This is consistent with the experimental observations that L_T/L_B are less than 1 in normal gravity (i.e. body forces are important). Bo reduces to 10^{-2} when the gravity reduces to $0.02 g_e$ which might lead one to expect more symmetric joints in low-gravity. The data shows, however, that in reduced gravity, the ratio, L_T/L_B , is somewhat greater than 1. A possible explanation for this observation is that there is insufficient time or driving force for solder to flow from one side of the joint to the other prior to solidification.

Finally, estimates of the Marangoni number (surface tension gradient forces to viscous forces), Ma , shown in equation 3 are of the order 0.1 for a 1 K temperature gradient over a length, $L_S = 1$ mm.

$$Ma = \frac{L_S}{\alpha\mu} \left(\frac{\partial\sigma}{\partial T} \right) dT \quad (3)$$

These surface tension gradient forces can produce surface flows on the order of 10 mm/s. These relatively high surface flows may have complex interactions with both bubbles and microstructure. Such Marangoni flows are largely independent of the length scales of the solder joint but are dependent on the heating configuration. During the first 3 flight weeks, heating configuration was the same (heat applied to the “top” of the joint), however, heating times were not precisely controlled between test operators and had some variations that have not been accounted for in the current results.

CONCLUSIONS

In summary, reduced gravitational forces have been shown to have a significant effect on both the geometry and porosity of solder joints at PTH length scales (~ mm). The increase in porosity is caused by bubbles which remain in the solder joint during solidification. Provided that the soldering is performed during the “quality” portions of the $0-g_e$ parabola, g-jitter likely reduces the net bubble transport from the joint. In partial gravity environments, acceleration levels much above Martian levels appear to generate sufficient buoyant force to eliminate any reduced gravity influences for solder joints at PTH length scales. The changes in joint geometry are likely due to reductions in the body forces. The unsteady acceleration environment has minimal effect on the solder joint geometry. However, the $0-g_e$ joints are not symmetric and, in fact, the leg-length ratios are opposite to the normal

gravity joints. In normal gravity, the bottom legs of the solder joint are larger than the top, the opposite is true in our $0-g_e$ results. Other factors must play a role in determining the solder joint shape - one possible explanation is insufficient time prior to solidification for solder to flow through the joint resulting in non-symmetric joints in reduced gravity. Further work is being conducted in these areas to help understand the implications of a reduced gravity environment on the soldering process.

REFERENCES

1. Winter, C. and Jones, J.C. 1996. The Microgravity Research Experiments (MICREX) Database, NASA TM-108523, <http://mgravity.itsc.uah.edu/microgravity/micrex/>.
2. Duffy, B., Personal Communication with J.K. Watson, 2000.
3. Pettegrew, R.D., Struk, P.M., Watson, J.K., and Haylett, D.R., Experimental Methods in Reduced-Gravity Soldering Research, NASA/TM—2002-211993. 2002.
4. Pettegrew, R.D., Struk, P.M., Watson, J.K., Haylett, D.R., and Downs, R.S., Gravitational Effects on Solder Joints, *Welding Journal*, pp. 44–48. October 2003.
5. Lekan, J., Neumann, E.S., and Sotos, R.G. Capabilities and Constraints of NASA’s Ground-Based Reduced Gravity Facilities, NASA CP-10113. 1992.
6. Boyer, E.O., Rieke, W.J., and Grodsinsky, C.M. Microgravity Research on the NASA Lewis Learjet Test Facility. 31st Aerospace Sciences Meeting and Exhibition, Reno, NV, AIAA-93-0573.
7. Ross, H.D. (ed), Microgravity Combustion: Fire in Free Fall. Academic Press. San Diego. pp. 18–21 (2001).
8. National Aeronautics and Space Administration. JSC Operations User’s Guide: JSC Reduced Gravity Program User’s Guide, Johnson Space Center, JSC Document 22803. May 2002.
9. Space Acceleration Measurement System (SAMS), <http://www.lerc.nasa.gov/WWW/MMAP/SAMSFF/#What>, 2003.

10. Fedor, G., Computer Engineer, ZIN Technologies, Cleveland, Ohio, Personal Communication with P.M. Struk, 2003.
11. ASTM Committee E-4. 2001. Standard Practice for Determining the Inclusion or Second-Phase Constituent Content of Metals by Automatic Image Analysis. Annual Book of ASTM Standards 2001 Sect. 3, Vol 03.01 July.
12. Woyczynski, W.A., Department of Statistics, Case Western Reserve University, Cleveland, Ohio, Personal Communication with P.M. Struk, 2003.
13. Sy, F., Taunton, J.W., and Lightfoot, E.N., AICHE J. 16 386-391. 1970.
14. Sy, F. and Lightfoot, E.N., AICHE J. 17, 177-181. 1971.
15. Morrison, F.A. and Stewart, M.B., *J. Appl. Mech.* 43, 399-403. 1976.
16. Clift, R., Grace, J.R., and Weber, M.E., Bubbles, Drops, and Particles, Academic Press, New York, Chapters 3 & 11. 1978.
17. Solder Alloy Data: Mechanical properties of solders and soldered joints, Inter. Tin Research Inst. Publication 656, p. 38. 1986.
18. Stokes, G.G., Trans. Cambridge Philos. Soc, 9, pp. 8-27. 1851.
19. Batchelor, G.K., Heat Transfer by Free Convection Across a Closed Cavity Between Vertical Boundaries at Different Temperatures, *Quart. J. Appl. Maths.* 12, pp. 209-233. 1954.

REPORT DOCUMENTATION PAGEForm Approved
OMB No. 0704-0188

Public reporting burden for this collection of information is estimated to average 1 hour per response, including the time for reviewing instructions, searching existing data sources, gathering and maintaining the data needed, and completing and reviewing the collection of information. Send comments regarding this burden estimate or any other aspect of this collection of information, including suggestions for reducing this burden, to Washington Headquarters Services, Directorate for Information Operations and Reports, 1215 Jefferson Davis Highway, Suite 1204, Arlington, VA 22202-4302, and to the Office of Management and Budget, Paperwork Reduction Project (0704-0188), Washington, DC 20503.

1. AGENCY USE ONLY (Leave blank)		2. REPORT DATE February 2004	3. REPORT TYPE AND DATES COVERED Technical Memorandum	
4. TITLE AND SUBTITLE The Effects of an Unsteady Reduced Gravity Environment on the Soldering Process			5. FUNDING NUMBERS WBS-22-101-58-10	
6. AUTHOR(S) Peter M. Struk, Richard D. Pettegrew, Robert S. Downs, and J. Kevin Watson				
7. PERFORMING ORGANIZATION NAME(S) AND ADDRESS(ES) National Aeronautics and Space Administration John H. Glenn Research Center at Lewis Field Cleveland, Ohio 44135-3191			8. PERFORMING ORGANIZATION REPORT NUMBER E-14386	
9. SPONSORING/MONITORING AGENCY NAME(S) AND ADDRESS(ES) National Aeronautics and Space Administration Washington, DC 20546-0001			10. SPONSORING/MONITORING AGENCY REPORT NUMBER NASA TM-2004-212946 AIAA-2004-1311	
11. SUPPLEMENTARY NOTES Prepared for the 42nd Aerospace Sciences Meeting and Exhibit sponsored by the American Institute of Aeronautics and Astronautics, Reno, Nevada, January 5-8, 2004. Peter M. Struk, NASA Glenn Research Center; Richard D. Pettegrew and Robert S. Downs, National Center for Microgravity Research, Cleveland, Ohio 44135; and J. Kevin Watson, NASA Johnson Space Center. Responsible person, Peter M. Struk, organization code 6711, 216-433-5948.				
12a. DISTRIBUTION/AVAILABILITY STATEMENT Unclassified - Unlimited Subject Categories: 29, 26, 14, and 34 Available electronically at http://gltrs.grc.nasa.gov This publication is available from the NASA Center for AeroSpace Information, 301-621-0390.			12b. DISTRIBUTION CODE	
13. ABSTRACT (Maximum 200 words) An improved understanding of the effects of reduced gravity is important to applications of soldering during both current and future human space missions. Recently, we conducted a series of manual soldering experiments aboard NASA's KC-135 reduced gravity aircraft. This paper focuses on the interpretation of the unsteady (g-jitter) acceleration environment measured aboard the aircraft as it affects the experimental results. The results presented here use a through-hole geometry that was soldered with the same hardware that is currently on orbit aboard the International Space Station. As presented elsewhere, we observed significant changes in porosity and geometry of solder joints formed in reduced gravity. Based on acceleration measurements during periods when the solder was molten, we examined a data filtering technique to determine the influence of g-jitter on our data. The results of this filter indicate that joint geometry is largely unaffected by the unsteady variations in acceleration as seen aboard the KC-135. We deduced that the increase in voids observed in low gravity can be described by decreases in buoyancy driven bubble motion. An acceleration environment which oscillates about zero gravity further increases joint porosity by keeping bubbles within the joint. Additionally, by examining some partial gravity results we observed that acceleration levels near Martian levels and higher result in porosity data sets similar to our normal gravity results. This suggests the existence of a "threshold" acceleration level below which gravitational effects become important for joint porosity in the through-hole geometry. The techniques and interpretations presented in this paper may be beneficial to others using the KC-135 research aircraft.				
14. SUBJECT TERMS Microgravity applications; Microgravity; Soldered joints; Soldering			15. NUMBER OF PAGES 17	
			16. PRICE CODE	
17. SECURITY CLASSIFICATION OF REPORT Unclassified	18. SECURITY CLASSIFICATION OF THIS PAGE Unclassified	19. SECURITY CLASSIFICATION OF ABSTRACT Unclassified	20. LIMITATION OF ABSTRACT	